

## Investigation of the skin effect in the bulk of electrical conductors with spin-polarized neutron radiography

I. Manke,<sup>1,a)</sup> N. Kardjilov,<sup>2</sup> M. Strobl,<sup>2</sup> A. Hilger,<sup>2</sup> and J. Banhart<sup>2</sup>

<sup>1</sup>*Institute of Materials Science and Technology, Technical University Berlin, Hardenbergstr. 36, 10623 Berlin, Germany*

<sup>2</sup>*Hahn-Meitner Institute Berlin, Glienicke Str. 100, 14109 Berlin, Germany*

(Received 3 June 2008; accepted 20 August 2008; published online 13 October 2008)

The skin effect in the bulk of an electrical conductor, i.e., the displacement of the current density from the inner part to the edges of a conductor, was investigated with spatial resolution using spin-polarized neutron imaging. Different current frequencies from 10 to 1000 Hz were applied to a sample. At each frequency the current distribution was analyzed and the influence of the electrical contacts was investigated. The experimental findings are in qualitative agreement with theoretical predictions and prove the suitability of spin-polarized neutron imaging as a unique tool for investigations of current density distributions in bulk materials in general. © 2008 American Institute of Physics. [DOI: 10.1063/1.2992516]

Knowledge of the electrical current distributions in conductors is important in many fields of research involving the development of electrical devices (e.g., transformers, inductors, electric motors, electric shielding materials), high current applications, loss-free interconnections, superconductive materials, batteries, fuel cells, or applications in plasma physics, to name a few.<sup>1–12</sup> In general the current distribution in a conductor depends strongly on the current frequency, the shape and size of the current function, and the shape and material of the conductor itself.<sup>1,13</sup> Electrical alternating currents in massive conductors have a tendency to be displaced from the core to the surface (skin) due to the interaction between eddy currents in different regions of the material. This phenomenon is known as the skin effect.<sup>1,2,6,13</sup> The skin effect results in a decrease in conductivity because it reduces the effective cross section for current transport.

For a cylindrical rod-shaped conductor the skin depth marks the depth below the surface of the conductor at which the current density has fallen to  $1/e$  of the value at the surface. The skin depth  $\delta$  can be calculated by

$$\delta = \sqrt{\frac{2\rho}{\omega\mu}}, \quad (1)$$

where  $\omega$  is the frequency of the applied alternating current,  $\rho$  is the resistivity of the conductor, and  $\mu$  is the absolute magnetic permeability of the conductor.<sup>1</sup>

Exact quantitative descriptions of current distributions are difficult to achieve and in practice very often impossible to calculate.<sup>1,14–16</sup> In particular, manufacturing tolerances, material inhomogeneities, or varying electrical contact qualities can introduce unpredictable effects.

Thus a method that provides spatially resolved experimental data, i.e., a complete image of the current distribution inside the bulk of the current conducting device is highly desirable. Here we demonstrate that imaging with spin-polarized neutrons enables the detection of the magnetic field

distribution around and—even more importantly—inside massive electrical conductors.<sup>17</sup> This method was applied to measure the skin effect in a reference sample at different frequencies.

Measurements were performed at the neutron imaging facility CONRAD at the Hahn-Meitner-Institut Berlin. A schematic drawing of the experimental setup is shown in Fig. 1. The monochromatic neutron beam was polarized by a solid state spin-polarizing bender,<sup>17</sup> and passed through the sample. The beam polarization was then analyzed by a second polarizing bender, the so-called spin analyzer, and transmitted neutrons were collected in a spatially resolving detector.<sup>17</sup>

In such a polarized neutron imaging setup the magnetic field of a sample provides image contrast due to changes in the previously defined neutron spin state that occurs in a magnetic field.<sup>17–19</sup> In the ideal case, the magnetic field to be visualized in and around a conductor is aligned perpendicular to the (initial) neutron spin polarization direction and the overall rotation of the neutron spin is not more than  $\pi$ . The transmission signal behind the spin analyzer at a location  $(x,y)$  in the detector plane is given by

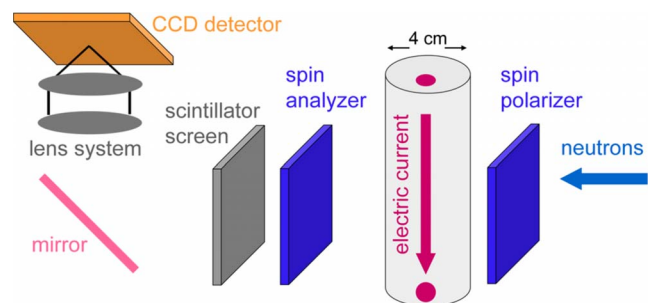


FIG. 1. (Color online) Schematic drawing of the experimental setup. An aluminum rod of 4 cm thickness with applied asymmetrical electric contact (top: 1 cm offset, bottom: contact at the side).

<sup>a)</sup>Electronic mail: manke@hmi.de.

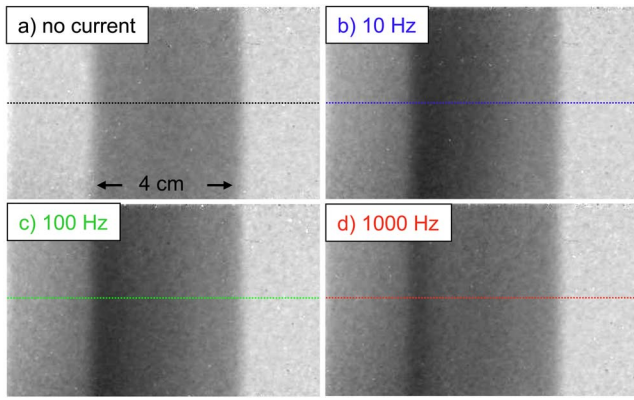


FIG. 2. (Color online) (a) Spin-polarized neutron radiograms (non-normalized raw data) of a 4 cm thick aluminum rod without applied current and with 25 A alternating current at (b) 10 Hz, (c) 100 Hz, and (d) 1000 Hz. Due to the asymmetric electric contact and the skin effect the current is shifted to the left side at increased frequencies resulting in a corresponding shift of the magnetic field.

$$I(x,y) = I_0(x,y) \exp \left[ - \int_{\text{path}} \Sigma(s) ds \right] \underbrace{\frac{1}{2} [1 + \cos \varphi(x,y)]}_{I_m(x,y)/I_0(x,y)} \quad (2)$$

where  $\varphi(x,y)$  is the angle between the analyzer orientation (which is parallel to the initial polarization direction) and the magnetic moment of the neutron,  $I_0(x,y)$  is the initial beam intensity, and  $\Sigma(s)$  is the linear attenuation coefficient of the sample along the path  $s$ .  $I_a(x,y)$  represents the conventional attenuation contrast and  $I_m(x,y)$  is the contrast variations due to spin rotation.

The current distribution in a conducting cylindrical aluminum rod with 4 cm diameter was investigated. Two electrical contacts were fixed to the rod at the top and bottom surfaces such that the magnetic field of the sample was perpendicular to the vertically oriented magnetic moment of the neutrons. For the first measurements the contacts were placed at different positions off the center of the circular cross section in order to simulate a realistic nontrivial case (Fig. 1). Images were taken with different applied currents. The exposure time for a single image was up to 120 s. The field of view was  $8 \times 3 \text{ cm}^2$  and the spatial resolution was approximately  $300 \text{ }\mu\text{m}$  in the vertical and  $500 \text{ }\mu\text{m}$  in the horizontal direction, mainly limited by the beam divergence.<sup>17</sup>

Figure 2(a) shows a radiogram of the aluminum rod without an applied current. The image contrast was due to the attenuation of the neutron beam by the aluminum only. No spin rotation occurred and the transmission of the polarization analyzer was at its maximum. When a current of 25 A was applied to the rod, a dark area that can be identified at the left hand side in Fig. 2(b) could be observed. This additional contrast was caused by the magnetic field induced by the current and the corresponding precession of the neutron spins around the field direction in this area. This result implies that the current flow was concentrated at the left side of the aluminum rod, which would be expected corresponding to the asymmetry of the electrical contact; the current indeed

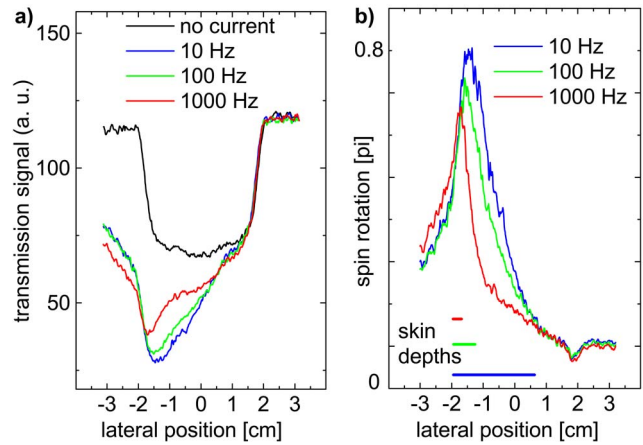


FIG. 3. (Color online) (a) Non-normalized cross sections along the marked lines in Figs. 2(a)–2(d). Without applied current only the attenuation by the aluminum rod is visible. With applied current the transmission signal is further decreased due to the neutron spin rotation. The gray shaded area marks the extensions of the aluminum rod. (b) The graphs in (a) were normalized and reveal the beam polarization. The values for the skin depth are shown for the three frequencies applied.

preferred the path with the least electrical resistance. However, as described above, in the case of alternating current the skin effect also has to be taken into account. In theory the actual current density distribution observed in the measurement can be derived by considering the current distribution for direct current, the effect of the skin depth, and the influence of the shape of the conductor and the contact areas. Due to the asymmetric electrical contact and the skin effect the current was shifted to the left side. An increase in the effect with increasing frequencies can be predicted and results in a corresponding shift of the magnetic field.

This can be seen in Fig. 3 where line profiles along the marked lines in Figs. 2(a)–2(d) are plotted. The line graphs are colored corresponding to the lines in Fig. 2. The gray shaded area marks the extension of the aluminum rod. In order to separate attenuation contrast and contrast caused by the spin analyses, the graphs were normalized by dividing them by an image of the sample with zero applied current. In this way the shift of the current toward the surface area as well as the narrowing of the magnetic field distribution at higher frequencies could be clearly visualized.

Although a straight-forward calculation of the current density distributions is impossible due to inherently unknown parameters, e.g., the exact contact area, it is interesting to compare at least the measured curves with the corresponding calculated skin depths at different frequencies, which are shown as lines of different lengths at the bottom in Fig. 3(b). Although this comparison is only qualitative, good agreement could be found between experiment and theory. At 10 Hz the calculated skin depth is 21 mm. A slight discrepancy in this case is due to the given geometry like contacting and the limited width of the sample itself.

In order to demonstrate the strong influence of the contact area of the rod another similar experiment was performed. The contact points were moved to the center of both faces of the rod, i.e., the electrical contact was symmetrical in this experiment. Figure 4(a) shows normalized radiograms

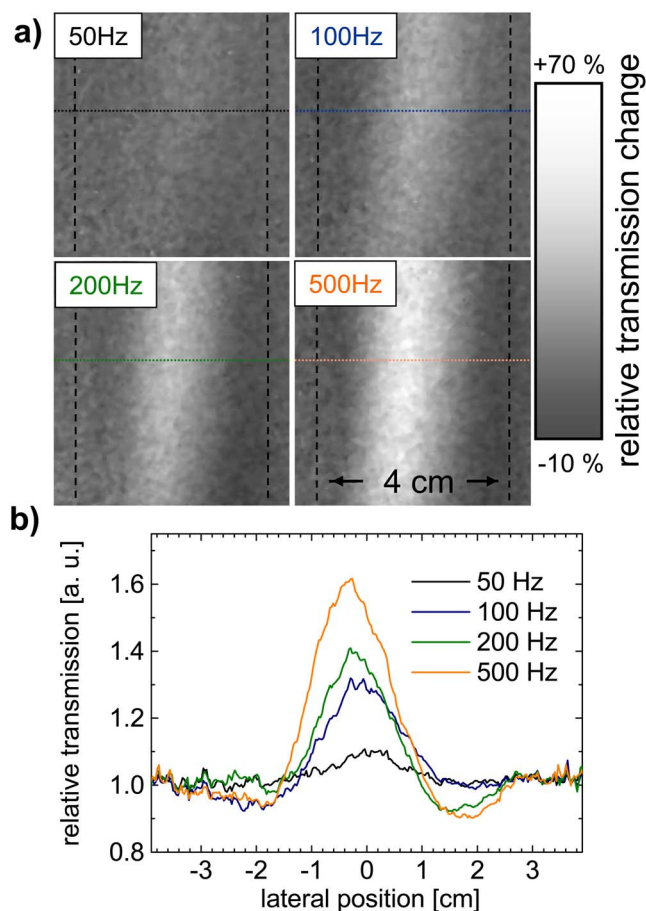


FIG. 4. (Color online) Normalized radiograms of a 4 cm aluminum rod as shown in Fig. 2, but with a symmetrical electrical contact at the top and bottom side.

from this series of measured images. However, in this case a slightly different normalization procedure was applied. Here the images have been normalized to an image taken at an alternating current with a very low frequency, 10 Hz. This way not only is the attenuation contrast eliminated, the differences in the magnetic field distributions to the case of the alternating current at 10 Hz remain.

When the magnetic field inside the aluminum rod is displaced toward the surface of the rod the rotation of the neutron polarization direction at the center of the image decreases because the integral magnetic field passed by the neutrons along the way through the sample is decreasing. Hence the (analyzer) transmission increases. In contrast, at the edges of the sample in the projection image neutrons have transmitted the increased (displaced) magnetic field and thus transmission decreases in these areas [see Eq. (2)]. Correspondingly, the images reveal that the current flow is squeezed almost equally outward, with the effect being stronger at higher frequencies, as may be expected. However, an asymmetry is found that is best visible in Fig. 4(b) where line profiles along the marked lines in Fig. 4(a) are shown; clearly the contact points are not perfectly symmetrical. The electrical contact across what is a large area (approximately  $1 \text{ cm}^2$ ) is not homogeneous. This asymmetry demonstrates that calculations alone would not have been sufficient to describe the current density flows in this simple conductor and

hence the results imply the need for measurements to investigate such effects in engineering devices.

Spin-polarized neutron imaging is a nondestructive and noninvasive method suitable to investigate magnetic field distributions in the bulk of conducting materials in order to determine the current density distribution. We have investigated the skin effect in an aluminum sample with a thickness of 4 cm at different alternating current frequencies. Results have been found to be in qualitative accordance with calculations of the skin depth but they clearly imply the superiority of and need for measurements in order to obtain reliable information. As an example the dependence on small variations in contacting has been demonstrated.

The achieved results suggest that the applied method of polarized neutron imaging is appropriate not only for investigating the skin effect even in complex conductors (e.g., Millikan conductors) but can be applied to visualize and investigate electrical currents in general, e.g., in fuel cells, in batteries, or in superconducting devices. Additionally it should be mentioned that the skin effect itself, which is influenced by cracks and other material inhomogeneities in conductors, can be exploited for imaging hidden cracks or other flaws.<sup>20–22</sup> Hence, applications in nondestructive testing of material properties, in device testing or even crack analysis in engineering components might also be promising.

The research activities were partially supported by the German Federal Ministry for Education and Science (BMBF) under Grant Nos. 03SF0324A and 03SF0324F.

- <sup>1</sup>W. A. Thue, *Electrical Power Cable Engineering*, 2nd ed. (Dekker, New York, 2003).
- <sup>2</sup>H. Saguy and D. Rittel, *Appl. Phys. Lett.* **89**, 094102 (2006).
- <sup>3</sup>A. Van den Bossche and V. C. Valchev, *J. Appl. Phys.* **97**, 10Q703 (2005).
- <sup>4</sup>A. W. Lotfi, P. M. Gradzki, and F. C. Lee, *IEEE Trans. Magn.* **28**, 2169 (1992).
- <sup>5</sup>N. Ando, *New Technics for Reduction of Transmission Loss in Power Cables*.
- <sup>6</sup>K. Sugiyama and K. Hayashida, *Hitachi Rev.* **30**, 51 (1981).
- <sup>7</sup>U. Fromm, *Euro. Trans. Electr. Power* **15**, 109 (2005).
- <sup>8</sup>D. Zhang and C. F. Foo, *Meas. Sci. Technol.* **10**, N44 (1999).
- <sup>9</sup>J. Guo, D. Kajfez, and A. W. Glisson, *Electron. Lett.* **33**, 966 (1997).
- <sup>10</sup>G. Cunge, B. Crowley, D. Vender, and M. M. Turner, *J. Appl. Phys.* **89**, 3580 (2001).
- <sup>11</sup>C. Hartnig, I. Manke, N. Kardjilov, A. Hilger, M. Grünerbel, J. Kaczerowski, J. Banhart, and W. Lehnert, *J. Power Sources* **176**, 452 (2008).
- <sup>12</sup>I. Manke, C. Hartnig, M. Grünerbel, J. Kaczerowski, W. Lehnert, N. Kardjilov, A. Hilger, W. Treimer, M. Strobl, and J. Banhart, *Appl. Phys. Lett.* **90**, 184101 (2007).
- <sup>13</sup>G. S. Smith, *Am. J. Phys.* **58**, 996 (1990).
- <sup>14</sup>J.-S. Wang, *IEEE Trans. Magn.* **32**, 1074 (1996).
- <sup>15</sup>J. Acero, R. Alonso, L. A. Barragán, and J. M. Burdío, *IEEE Trans. Magn.* **42**, 2152 (2006).
- <sup>16</sup>A. W. Lotfi, P. M. Gradzki, and F. C. Lee, *IEEE Trans. Magn.* **28**, 2169 (1992).
- <sup>17</sup>N. Kardjilov, I. Manke, M. Strobl, A. Hilger, W. Treimer, M. Meissner, T. Krist, and J. Banhart, *Nat. Phys.* **4**, 399 (2008).
- <sup>18</sup>E. Lehmann and N. Kardjilov, in *Advanced Tomographic Methods in Materials Research and Engineering*, edited by J. Banhart (Oxford University, New York, 2008), p. 375.
- <sup>19</sup>E. Jericha, R. Szeywerth, H. Leeb, and G. Badurek, *Physica B (Amsterdam)* **397**, 159 (2007).
- <sup>20</sup>H. Saguy and D. Rittel, *Appl. Phys. Lett.* **91**, 084104 (2007).
- <sup>21</sup>Q. Wen and D. R. Clarke, *J. Appl. Phys.* **83**, 1132 (1998).
- <sup>22</sup>M. P. Hentschel, private communications.